UCSF
UC San Francisco Previously Published Works

Title

BMPR2 Preserves Mitochondrial Function and DNA during Reoxygenation to Promote Endothelial Cell Survival and Reverse Pulmonary Hypertension

Permalink

https://escholarship.org/uc/item/0fn624n9

Journal

Cell Metabolism, 21(4)

ISSN

1550-4131

Authors

Diebold, Isabel
Hennigs, Jan K
Miyagawa, Kazuya
et al.

Publication Date

2015-04-01

DOI

10.1016/j.cmet.2015.03.010

Peer reviewed

BMPR2 Preserves Mitochondrial Function and DNA Integrity During Reoxygenation to Promote Endothelial Survival and Reverse Pulmonary Hypertension

Isabel Diebold[*,§], **Jan K. Hennigs**[*,§], **Kazuya Miyagawa**[*,§], **Caiyun G. Li**[*,§], **Nils P. Nickel**[*,§], **Mark Kaschwich**[*,§], **Aiqin Cao**[*,§], **Lingli Wang**[*,§], **Sushma Reddy**[*], **Pin-I Chen**[*,§], **Kiichi Nakahira**[†], **Miguel A. Alejandre Alcazar**[*,§], **Rachel K. Hopper**[*,§], **Lijuan Ji**[*], **Brian J. Feldman**[*], and **Marlene Rabinovitch**[*,§]

[*]Department of Pediatrics, Cardiovascular Institute, Stanford University School of Medicine, Stanford, CA 94305

[§]The Vera Moulton Wall Center for Pulmonary Vascular Disease, Stanford University School of Medicine, Stanford, CA 94305

[†]Department of Medicine, Weill Cornell Medical College, New York, NY 10065, USA

Summary

Mitochondrial dysfunction, inflammation and mutant bone morphogenetic protein receptor (BMPR)2 are associated with pulmonary arterial hypertension (PAH), an incurable disease characterized by pulmonary arterial (PA) endothelial cell (EC) apoptosis, decreased microvessels and occlusive vascular remodeling. We hypothesized that reduced BMPR2 induces PAEC mitochondrial dysfunction, promoting a pro-inflammatory or pro-apoptotic state. Mice with EC-deletion of BMPR2 develop hypoxia-induced pulmonary hypertension that, in contrast to non-transgenic littermates, does not reverse upon reoxygenation and is associated with reduced PA microvessels and lung EC p53, PGC1α and TFAM, regulators of mitochondrial biogenesis and mitochondrial DNA. Decreasing PAEC BMPR2 by siRNA during reoxygenation represses p53, PGC1α, NRF2, TFAM, mitochondrial membrane potential and ATP and induces mitochondrial DNA deletion and apoptosis. Reducing PAEC BMPR2 in normoxia increases p53, PGC1α, TFAM, mitochondrial membrane potential, ATP production and glycolysis, induces mitochondrial

fission, and a pro-inflammatory state. These features are recapitulated in PAEC from PAH patients with mutant BMPR2.

Introduction

Endothelial cells (EC) are continually exposed to injurious stimuli that adversely affect their interaction with platelets and inflammatory cells, alter their permeability, dysregulate their inhibition of smooth muscle cell (SMC) proliferation, and even induce apoptosis (Park et al., 2013). The ability of EC to withstand these insults relies upon the energetic machinery of the mitochondria. The influence of reoxygenation following hypoxia (hypoxia-reoxygenation) on EC mitochondrial function has been studied in many vascular beds, including the lung, where the most profound alterations occur (Giedt et al., 2012). Common examples of hypoxia-reoxygenation include exposure to and return from high altitude. Pathological conditions include lung infections, acute respiratory distress syndrome in adults and premature neonates (Matuschak et al., 1998), and administration of oxygen during anesthesia and in the postoperative setting. Chronic hypoxia-reoxygenation underlies recurrent pulmonary thromboembolism and sleep apnea. In the vast majority of individuals, adaptation to hypoxia-reoxygenation is not a problem. However failure of normal mitochondrial adaptation to hypoxia-reoxygenation could play a role in EC dysfunction related to PAH (Jilwan et al., 2013), pulmonary edema, or inflammation causing fibrosis (Gill et al., 2014).

Altered mitochondrial metabolism associated with glycolysis was described in PAH (Archer et al., 2008; Michelakis et al., 2002b; Ryan et al., 2013). Specific mitochondrial abnormalities related to clinical PAH and experimental pulmonary hypertension (PH) include induction of a pseudohypoxic state via activation of hypoxia-inducible factor 1α (HIF1α), impaired mitochondrial-endoplasmic reticulum interaction, and mitochondrial fission (Fijalkowska et al., 2010; Sutendra and Michelakis, 2014). Dysmorphic mitochondria with defects in the electron transport chain, lower respiratory chain coupling and inefficient use of oxygen have also been reported (Michelakis et al., 2002b; Xu et al., 2007). These abnormalities were linked to the chronic inflammatory process in PAH (Sutendra et al., 2011) and to the progressive expansion of SMC-like cells that obliterate the vascular lumen (Teichert-Kuliszewska et al., 2006).

Mitochondrial dysfunction has been most extensively investigated in vascular SMC (Michelakis et al., 2002a; Sutendra et al., 2010). However, PAEC from PAH patients are also characterized by aberrant mitochondrial function and a glycolytic state (Masri et al., 2007; Xu et al., 2007) and EC dysfunction is central to the pathological changes that increase pulmonary vascular resistance. For example, vulnerability of PAEC to apoptosis is related to loss of distal pulmonary vessels (Teichert-Kuliszewska et al., 2006) and emergence of apoptosis-resistant PAEC in advanced occlusive plexogenic lesions (Sakao et al., 2009). EC dysfunction also impairs production of factors such as apelin that repress SMC proliferation (Alastalo et al., 2011; Kim et al., 2013).

PAEC dysfunction in PAH has been related to a mutation in the bone morphogenetic protein receptor 2 (*BMPR2*) gene, found in approximately 70% of families with PAH (Deng et al.,

2000; Lane et al., 2000) and in 20% of sporadic cases of idiopathic (I) PAH. Impaired BMPR2 signaling is linked to the propensity of PAEC to apoptose (Alastalo et al., 2011; Teichert-Kuliszewska et al., 2006), and to amplification of a pro-inflammatory state (Sawada et al., 2014a). As reduced BMPR2 expression, independent of a mutation, is a feature of PAH (Atkinson et al., 2002), we hypothesized a direct link between abnormal activity of BMPR2 and impaired mitochondrial function.

Since BMPR2 regulates peroxisome proliferator-activated receptor-γ (PPARγ)-mediated gene transcription in EC and SMC (Guignabert et al., 2009; Hansmann et al., 2008), we postulated that the PPARγ co-activator (PGC1α), that plays a key role in mitochondrial biogenesis (Ryan et al., 2013) would also be regulated by BMPR2. PGC1α dysfunction is linked to various cardiovascular diseases (Rowe et al., 2010; Ryan et al., 2013; Sawada et al., 2014b). Recent reports implicate the tumor suppressor p53 in regulating PGC1α in neuroblastoma cells, cardiomyocytes and EC (Aquilano et al., 2013; Shimasaki et al., 2013; Villeneuve et al., 2013). PGC1α is also a co-activator of the transcription factors NRF1/2, that control the expression of genes encoding antioxidant enzymes and mitochondrial DNA (mtDNA) replication, such as the mitochondrial transcription factor A (TFAM) (Scarpulla, 2008).

In this study we investigated transgenic mice with deletion of *Bmpr2* in EC, normal human PAEC with BMPR2 depleted by siRNA, and PAEC from PAH patients with mutant *BMPR2*. Under basal conditions, loss of PAEC BMPR2 causes an aberrant increase in mitochondrial membrane potential and a pro-inflammatory state. However, during hypoxia-reoxygenation, reduced BMPR2 decreases mitochondrial biogenesis and energy metabolism and promotes mtDNA damage and EC apoptosis.

Results

Mice with *Bmpr2* deleted in endothelial cells have sustained pulmonary hypertension following hypoxia-reoxygenation, associated with mitochondrial dysfunction

To establish a relationship between reduced BMPR2, mitochondrial dysfunction and PH, we used transgenic mice in which *Bmpr2* was deleted in EC (EC-*Bmpr2*$^{-/-}$). These mice were produced by breeding SCL-*Cre*ER™, R26*LacZ*$^{fl/fl}$ and *BMPR2*$^{fl/fl}$ mice, to create conditional EC-specific *Bmpr2* knockout (KO) mice following a 10-day injection of tamoxifen and were characterized by our group (Spiekerkoetter et al., 2013). They show no significant PH at baseline and only a modest increase, relative to wild type littermates (WT), following chronic hypoxia, as judged by right ventricular systolic pressure (RVSP) and right ventricular hypertrophy (RVH) (Spiekerkoetter et al., 2013). However, we now report a more impressive phenotype following an additional mitochondrial challenge, reoxygenation following hypoxia. When KO mice were returned to room air for one month after a prior three-week exposure to chronic hypoxia (10% oxygen), they showed a pronounced increase in RVSP when compared to WT mice where values normalized to pre-hypoxia control levels (Fig. 1A). Consistent with this, KO mice had markedly reduced PA acceleration time (PAAT) assessed by transthoracic echocardiography (Fig. S1A). WT mice showed only a modest reduction in PAAT after hypoxia-reoxygenation, perhaps slightly overestimating PA pressure due to the limited sensitivity of the technique (Urboniene et al., 2010). No

differences were observed in heart rate, cardiac output or ventricular function across genotypes or experimental conditions (Fig. S1B–D), indicating that the RV maintains contractility despite the higher RVSP. This would suggest that deletion of BMPR2 in coronary artery EC during hypoxia-reoxygenation does not impact cardiac function during the time frame studied.

Consistent with the hemodynamic data, KO mice in hypoxia-reoxygenation vs. WT also showed persistent RVH (Fig. 1B), enhanced muscularization of distal pulmonary arteries (DPA) (Fig. 1C and Fig. S1E), and reduced number of DPA per 100 alveoli (Fig. 1D). Since the severity of reduced DPA in both genotypes was similar after hypoxia (Spiekerkoetter et al., 2013), our data suggest that the KO mice have an impaired capacity to regenerate DPA. In fact, lung EC isolated from KO mice after hypoxia-reoxygenation vs. WT mice, showed a pro-apoptotic phenotype, judged by increased caspase 3/7 activity (Fig. 1E). Migration of lung EC from KO mice was impaired (Fig. S1F) as was tube formation in Matrigel (Fig. S1G). These features are consistent with compromised regeneration of DPA in hypoxia-reoxygenation.

Abnormalities in PAEC and mitochondrial function were linked. Compared to WT littermates, lung EC from KO mice in normoxia showed elevated reactive oxygen species (ROS) assessed by dihyidroethidium (DHE), and MitoSox Red staining (Fig. 1F,G), indicating that the source of ROS was mitochondrial. The reduction in mitochondrial ROS during hypoxia-reoxygenation was more pronounced in KO vs. WT mice. KO mice also showed an increase in mitochondrial membrane potential (ψ_m) in normoxia, and a severe reduction following hypoxia-reoxygenation (Fig. 1H) as assessed by JC-1 or TMRE fluorescence. However, PASMC isolated from EC-$Bmpr2^{-/-}$ and WT mice, showed a similar reduction in ψ_m following hypoxia-reoxygenation (Fig. S1H).

To determine whether the changes in ψ_m reflected altered mitochondrial biogenesis, we assessed protein levels of PGC1α and of p53, a known regulator of PGC1α (Villeneuve et al., 2013). p53 and PGC1α were increased by immunoblot in cultured lung EC of KO vs. WT mice in normoxia (Fig. 1 I, J); however, during hypoxia-reoxygenation, p53 levels fell relative to WT controls and PGC1α was reduced below WT levels in lung EC from the KO mice. Since PGC1α directs mtDNA replication via the transcription factor NRF2 and its target, TFAM (Virbasius and Scarpulla, 1994), we assessed TFAM protein levels. Like PGC1α, it was increased in lung EC of KO vs. WT mice in normoxia but was reduced after hypoxia-reoxygenation (Fig. 1K).

p53 and PGC1α related to altered BMPR2 in pulmonary artery endothelial cells

To understand the mechanism linking loss of BMPR2 with altered mitochondrial function and to extend our findings beyond the KO mouse, we carried out experiments on human PAEC transfected with control non-targeting or BMPR2 siRNA. Levels of BMPR2 mRNA and protein were reduced to about 20% of the levels in PAEC transfected with control siRNA. The PAEC were then either maintained in normoxia for 96h, in hypoxia (0.5% O_2) for 48h or 96h, or exposed to 48h of hypoxia followed by reoxygenation in normoxia for 48h.

Human PAEC transfected with BMPR2 siRNA vs. control siRNA, showed increased p53 and PGC1α whereas under hypoxia-reoxygenation, a decrease in p53 and PGC1α below normoxia levels was evident (Fig. 2A). Depletion of BMPR2 by siRNA resulted in an increase of p53 transcriptional activity under normoxia and a decrease in response to hypoxia-reoxygenation, paralleling our findings related to PGC1α and consistent with transcriptional regulation of PGC1α by p53 (Fig. S2A). Importantly, down-regulation of p53 by siRNA had no effect on the level of BMPR2 (Fig. S2B), indicating that p53 is downstream of BMPR2 signaling. Depletion of p53 by siRNA reduced PGC1α protein under both normoxia and hypoxia-reoxygenation (Fig. 2B), and depletion of both BMPR2 and p53 reduced PGC1α protein (Fig. 2C) and mRNA (Fig. S2B). All these data are consistent with regulation of PGC1α by p53. Surprisingly despite the increase in PGC1α protein with loss of BMPR2 there was no elevation in PGC1α mRNA (Figure S2C). This suggests that either that there was impaired stability of the PGC1α mRNA associated with loss of BMPR2 and enhanced p53 transcriptional activity, or that the increase in PGC1α protein associated with loss of BMPR2 is p53 dependent but not transcriptionally regulated. Also it is possible although less likely, that while basal production of PGC1α is p53 dependent, the augmentation that occurs with loss of BMPR2 is related to a different mechanism.

To evaluate whether the BMPR2-dependent regulation of p53 and PGC1α is relevant to non-PA EC, we reduced BMPR2 in human umbilical vein EC (HUVEC) and found BMPR2-dependent changes similar to those seen in PAEC (Fig. S2D). We established that HIF1α was upregulated during 48 and 96h of hypoxia but unaffected by loss of BMPR2 (Fig S2E). In response to 48 or 96h of hypoxia p53 levels fell, but independent of loss of BMPR2 (Fig. S2F).

To test the relevance of this pathway to ψ_m, we reduced BMPR2, p53 and PGC1α by siRNA in PAEC maintained in normoxia or hypoxia-reoxygenation, and determined ψ_m by JC-1 and TMRE assays. Loss of BMPR2 increased ψ_m under normoxia, and further reduced ψ_m during hypoxia-reoxygenation compared to control siRNA transfected PAEC (Fig. 2D). Decreasing either p53 or PGC1α reduced ψ_m under both normoxia and hypoxia-reoxygenation (Fig. 2E,F). In contrast, in human PASMC, ψ_m did not increase with loss of BMPR2 in normoxia, but did significantly increase in response to hypoxia-reoxygenation (Fig. S2G). This is consistent with studies showing hyperpolarized mitochondria in PAH PASMC (Sutendra and Michelakis, 2014) and suggests loss of BMPR2 function and another 'hit', e.g., reoxygenation following hypoxia, are necessary to increase ψ_m in PASMC.

Since mitochondrial function reflected in ψ_m is related to EC survival, we determined the impact of loss of BMPR2, p53 and PGC1α on the pro-apoptotic state of PAEC by the caspase-3/7 activity assay (Fig. 2G–I) as well as by Sub G1 FACS analysis using propidium iodide (Fig. S2H). Loss of BMPR2 significantly increased caspase activity and reduced the number of viable cells in hypoxia-reoxygenation (Fig. 2G and Fig S2H). Importantly, reducing p53 or PGC1α increased caspase activity under both conditions (Fig. 2H, I), suggesting a pro-survival role of p53 and PGC1α in PAEC as previously reported (Heo et al., 2011). BrdU incorporation revealed no BMPR2-dependent effect on proliferation in normoxia or hypoxia-reoxygenation (Fig S2I).

Reduced BMPR2 in normoxia creates a pro-inflammatory state in pulmonary artery endothelial cells

As in the lung EC from KO mice, we observed a significant increase in ROS production in PAEC with loss of BMPR2 under normoxia, whereas ROS was reduced below normoxia levels in response to hypoxia-reoxygenation in both control and BMPR2 siRNA treated cells (Fig. 3A). To confirm that the increase in ROS resulting from loss of BMPR2 under normoxia is mediated by mitochondrial respiration, we pre-treated BMPR2-depleted PAEC with Antimycin, a quinone analog that binds to cytochrome b_{562} and blocks electron transport to the ubiquinone in complex III. When pretreated with Antimycin, the ROS generated in response to reduced BMPR2 was no longer apparent and residual ROS was similar to that in control cells treated with Antimycin (Fig. 3B). We assessed whether the increase in mitochondrial ROS with depletion of BMPR2 in PAEC could be mediating an increase in mRNA expression of the pro-inflammatory cytokines Interleukin (IL)8 and IL6 (Fig. 3C,D). However, IL8 and IL6 were even further increased by Antimycin (Fig. 3E). TFAM may repair the mtDNA (Julian et al., 2013) and attenuate the inflammasome response involving IL8 and TLR-9 as reviewed in (West et al., 2011). Consistent with this, repression of TFAM by siRNA also further increased IL8 (Fig. 3F), This suggests that both the increase in ROS and in TFAM mitigate the inflammatory response.

PGC1α mediates activation of NRF2 and TFAM in pulmonary artery endothelial cells: Impact on mitochondrial DNA

TFAM is essential for mtDNA replication as well as maintenance and repair (Larsson et al., 1998). We documented only a trend toward an elevation in TFAM in PAEC with loss of BMPR2 during normoxia but a marked reduction with hypoxia-reoxygenation (Fig. 4A). Decreasing either PGC1α or NRF2 by siRNA reduced TFAM in normoxia and hypoxia-reoxygenation (Fig. 4B,C) whereas reducing NRF1 did not significantly affect TFAM levels (Fig. S3A). This is consistent with an increase in NRF2 transcriptional activity with loss of BMPR2 in normoxia, and a decrease with loss of BMPR2 and PGC1α with hypoxia-reoxygenation (Fig. S3B,C). Indeed, PGC1α siRNA reduces NRF2 transcriptional activity during both normoxia and hypoxia-reoxygenation (Fig. S3C). The reduced TFAM in hypoxia-reoxygenation was associated with loss of mtDNA (Fig. 4D).

We identified mitochondrial fission in cells lacking BMPR2 under normoxia that was further enhanced in hypoxia-reoxygenation (Fig. 4E). Since the balance between fission and fusion is important in maintaining mitochondrial integrity we investigated whether proteins known to regulate mitochondrial fusion, Mitofusin 1 and 2, are reduced by BMPR2 signaling in PAEC. Interestingly, both Mitofusin 1 and 2 were reduced but only in hypoxia-reoxygenation, and not aggravated by loss of BMPR2 (Fig. S3D,E). Mitophagy as assessed by LC3B protein level was also decreased during hypoxia-reoxygenation and unaffected by reduced BMPR2 (Fig. S3F).

The somatic mutation rate of mtDNA is 10–20 times higher than that of nuclear DNA (Taylor and Turnbull, 2005), and of particular interest is the induction of a large 4977bp deletion in mtDNA, (mtDNA^{4977}) associated with cancer and neurodegenerative diseases (Chen et al., 2011). The presence of mtDNA^{4977} was assessed by PCR-based amplification

of a specific 352bp amplicon that was validated by DNA sequencing. In cells lacking BMPR2 an increase in the amplicon (Fig. 4F) during hypoxia-reoxygenation was confirmed by qPCR (Fig. 4G). Reducing either PGC1α or TFAM under normoxia or hypoxia-reoxygenation did not induce an increase in mtDNA^{4977} (Fig. S3G) suggesting that additional factors related to reduced p53 are required.

To determine whether loss of TFAM mimicked reduced BMPR2 in producing a pro-apoptotic state, we assayed caspase activity in PAEC transfected with TFAM siRNA (Fig. 4H). Indeed, PAEC with reduced TFAM showed the same pro-apoptotic activity observed in cells with reduced BMPR2, but only in hypoxia-reoxygenation, indicating that loss of TFAM is necessary but that induction of apoptosis may require additional sequelae of reducing PGC1α.

To determine how reduced BMPR2 might influence mitochondrial metabolism we carried out an extracellular flux assay, using the SeaHorse system described in the Supplementary Methods. Under normoxia, in keeping with a high ψ$_m$ and ROS generation in PAEC with reduced BMPR2, there was an increase in oxygen consumption and derived mitochondrial ATP production. With hypoxia-reoxygenation, control PAEC also showed heightened mitochondrial ATP production and oxygen consumption but not PAEC with reduced BMPR2 (Fig. 5 A–D). Increased glycolysis and glycolytic reserve accompanied the increase in ATP production and oxygen consumption in both PAEC with loss of BMPR2 and in control siRNA PAEC under hypoxia-reoxygenation (Culic et al., 1997), (Fig. 5 E–G). However, under hypoxia-reoxygenation PAEC with reduced BMPR2 showed decreased mitochondrial respiration (ATP production) and a diminished glycolytic reserve.

The response to BMPR2 siRNA is recapitulated in pulmonary arterial endothelial cells from patients with a BMPR2 mutation and pulmonary arterial hypertension

To establish the clinical relevance of our findings to PAH patients, we assessed levels of BMPR2, p53, PGC1α, TFAM and the mtDNA^{4977} in cultured PAEC from three PAH patients, all with loss of function mutations of BMPR2 but with variable degrees of expression of the receptor (see Table S1 for characteristics of the patients and controls). As in the BMPR2 siRNA experiments, in PAEC from these patients vs. controls, p53, PGC1α and TFAM (Fig. 6 A–C) were elevated under normoxia, and decreased in hypoxia-reoxygenation. Although PAH PAEC showed an increase in ψ$_m$ in normoxia and a reduction in hypoxia-reoxygenation (Fig. 6D) there were no significant changes in ROS (Fig. 6E). This suggests either that mitochondrial ROS production is not a consistent by-product of the changes in mitochondrial metabolism related to membrane potential or that other ROS generating cellular processes in the PAH cells obscure the increase in mitochondrial ROS. There was an increase in the mtDNA^{4977} in the PAH PAEC in hypoxia-reoxygenation (Fig. 6F), and a pro-apoptotic state evident by an increase in caspase activity (Fig. 6G).

In keeping with our findings in human PAEC with reduced BMPR2, IL8 levels were increased in PAH PAEC in normoxia and reduced in hypoxia-reoxygenation (Fig. 6H). Interestingly, IL8 levels were also elevated in donor PAEC in hypoxia-reoxygenation, perhaps reflecting the inflamed state of cells harvested within 24h from our controls -

unused donor lungs that were excluded from transplant. As Toll-like receptor 9 (TLR9) can be activated by mtDNA to initiate the innate immune system (Zhang et al., 2010), consistent with an inflammasome response, we pre-treated PAH PAEC with the TLR9-inhibitor (ODN TTAGG) and observed a reduction in IL8 mRNA levels (Fig. 6I).

Discussion

Our studies using mice with BMPR2 deleted in lung EC, human PAEC with BMPR2 reduced by siRNA, and PAEC from PAH patients with mutant BMPR2 establish a connection between a known genetic abnormality linked to PAH and pathways that promote mitochondrial dysfunction and mtDNA damage. Loss of BMPR2 increases p53 transcriptional activity and PGC1α, NRF2 and TFAM, ψ_m mitochondrial ATP production and glycolysis. Mitochondria undergo fission and there is increased production of cytokines consistent with an inflammasome response (Julian et al., 2013). Conversely, PAEC with loss of BMPR2 respond to hypoxia-reoxygenation by repression of the p53-PGC1α-NRF2-TFAM pathway, lowering of ψ_m, failure to increase ATP production, and accumulation of a mtDNA deletion ($mtDNA^{4977}$), resulting in a propensity to apoptosis (Fig. 7). Both the decline in p53 transcriptional activity and the loss of ATP can contribute to the apoptosis of PAEC.

Apoptotic PAEC are linked to the pathogenesis of PAH related to loss of distal pulmonary arteries and to impaired production of EC factors that repress SMC growth (Alastalo et al., 2011; Chun et al., 2008). The 'pro-inflammatory' PAEC phenotype with loss of BMPR2 observed in these studies would facilitate infiltration of immune cells that contribute to occlusion of the vessel lumen (Sawada et al., 2014a). The fact that systemic EC exhibit the same mitochondrial abnormalities as PAEC in response to loss of BMPR2 further reinforces the importance of the pathway and is in keeping with studies showing abnormalities of microvessels in skeletal muscle in patients with PAH (Potus et al., 2014). The hypoxia-reoxygenation environment of the lung relative to other vascular beds would likely bring out the vulnerability of PAEC. In fact mutant BMPR2 also causes experimental PH in response to hyperoxia-induced mitochondrial injury (Fessel et al., 2013).

While our studies in PAH PAEC focused on those with a BMPR2 mutation, reduced expression or function of the receptor has been related to all forms of PAH (Atkinson et al., 2002) so we anticipate seeing similar abnormalities in gene regulation and mitochondrial function. It appears that it is the reoxygenation following hypoxia, not hypoxia per se, that may be the greater challenge to mitochondrial function, explaining why the phenotype of unresolved PH is more striking than the relatively mild exaggerated hypoxia-induced PH described in the KO mice (Spiekerkoetter et al., 2013). This could mean that the inability to reverse PH after a given perturbation may be more tightly linked to a genetic abnormality than the nature of the insult or the severity of the initial response to the perturbation. Alternatively there are genotype related changes that occur during hypoxia independent of p53 and HIF1α we did not measure, that underlie the response to hypoxia-reoxygenation. While it is possible that PH in the KO mice will regress over time, previous studies in rats indicate that virtually all of the recovery takes place in the first month of reoxygenation following hypoxia (Rabinovitch et al., 1981). Since mitochondrial changes in lung EC from

KO vs. WT are evident one month after hypoxia-reoxygenation and following passage in culture, the switch in cell phenotype is likely permanent. It would be interesting to pursue the role of epigenetics in maintaining this switch since changes in epigenetic factors are linked to altered mitochondrial metabolism in PH fibroblasts (Li et al., 2011) and SMC (Archer et al., 2010). In view of the abnormalities in mitochondrial metabolism described here and by others (Xu et al., 2007), therapies like dichloroacetate that normalize glucose oxidation by inhibiting pyruvate dehydrogenase kinase may be effective in reversing the phenotype of PAH PAEC (McMurtry et al., 2004; Michelakis et al., 2002b).

The opposing responses to loss of BMPR2 in normoxia and hypoxia-reoxygenation, i.e., heightened vs. reduced transcriptional activity of p53 and PGC1α, likely result from changes in intracellular signaling (Davies et al., 2012; O'Prey et al., 2010; Sawada et al., 2014a). Although Mizuno et al. (2011) reported an interaction between p53 and HIF1α in SMC, we could not detect BMPR2-dependent regulation of HIF1α under normoxia, hypoxia, or hypoxia-reoxygenation. Consistent with our findings that lung EC dysfunction and apoptosis in EC-$Bmpr2^{-/-}$ mice are coupled to heightened muscularization of distal arteries, p53 KO mice have increased proliferation of SMC and develop greater PH than WT mice during chronic hypoxia (Mizuno et al., 2011). Conversely, activation of p53 by the MDM2 inhibitor nutlin-3a prevents abnormal SMC proliferation associated with hypoxia-induced PH (Mouraret et al., 2013).

Under normoxia, reduced BMPR2 in PAEC increases ψ_m and ROS, consistent with similar results in PASMC transfected with mutant BMPR2 (Lane et al., 2011), but not in PASMC with BMPR2 siRNA, except under hypoxia-reoxygenation. NADPH oxidases are important sources of ROS in EC (Diebold et al., 2009), but do not appear to account for the BMPR2 deficient response. Reduced BMPR2 in PAEC caused heightened expression of IL6 and IL8 that was not ROS dependent but may relate to the changes in ψ_m and mitochondrial fission. In mice with genetic ablation of EC BMPR2, attenuation of leukocyte recruitment by blocking IL6 and IL8 receptors stops progression of PH (Burton et al., 2011).

Several studies have shown that accumulation of mtDNA[4977] is due to oxidative damage, caused by proximity of mtDNA to the ROS-producing respiratory chain and to the lack of effective repair mechanisms within mitochondria (Cheng et al., 2013). In BMPR2-deficient PAEC exposed to hypoxia-reoxygenation, accumulation of mtDNA[4977] is also seen with a decrease in ROS production. Recent studies reported that reduced Mitofusin-2 in PASMC contributes to disruption of mitochondria in PAH (Bonnet et al., 2006; Ryan et al., 2013). We found reduced Mitofusin-2 and Mitofusin-1 after hypoxia-reoxygenation but no BMPR2 related differences. It would be interesting to investigate other genes such as optic atrophy 1 (OPA1) that regulate mitochondrial fusion in cardiomyocytes (Duvezin-Caubet et al., 2006) or Dynamin-Related Protein 1 (DRP-1), a mediator of mitochondrial fission and apoptosis (Frank et al., 2001).

The pathway we identified, linking mitochondrial function to PAEC survival and BMPR2 signaling, could be important in developing therapies for PAH and other lung conditions with EC dysfunction. Our data suggest that even mild forms of intermittent hypoxia when coupled with dysfunction of BMPR2, may, by compromising mitochondrial adaptation,

promote the development, persistence or progression of PAH or cause other lung disorders related to PAEC dysfunction. Addressing the impact of oxygen administration in the presence of BMPR2 dysfunction, would also be of potential clinical importance. The pathway we have described may be relevant in other cells, e.g., in cancer, where germline mutations of the BMP pathway have been identified (Howe et al., 2001). Conversely a p53 mutation could be a modifier of PAH.

Experimental Procedures

Expanded experimental procedures are described in the Supplement

Mouse and Human Pulmonary Artery Endothelial Cells—Primary murine lung EC of WT or EC-*Bmpr2*$^{/-}$ mice were harvested from lung tissue by Elastase/Collagenase digestion (Kim et al., 2011) and isolated using CD31 antibody-coated magnetic beads (Alastalo et al., 2011). Primary human PAEC were commercially obtained. Additional primary PAEC were obtained from lungs removed at transplantation from PAH patients with a known BMPR2 mutation, and from unused donor lungs as controls (patient and donor characteristics in Table S1) (Sawada et al., 2014a). PAEC (passages 4–7) were grown in complete EC media. Human umbilical vein endothelial cells (HUVEC) were used at passages 3–5. For studies examining the response to hypoxia-reoxygenation, human PAEC, murine lung EC or HEK-293T cells were incubated in normoxia (21% O_2 5% CO_2) for 96h or under hypoxia (0.5% O_2, 5% CO_2) in a hypoxic workstation (In vivo$_2$ 400, Ruskinn Technology Microaerobic System) for 48h followed by re-incubation in normoxia (21% O_2 5% CO_2) for 48h. Medium was changed every 48h.

Mouse Pulmonary Artery Smooth Muscle Cells (PASMC)—Mouse PASMC were isolated using a modified Elastase/Collagenase digestion protocol (Kim et al., 2011).

Mouse Model—Cell-specific inducible EC-*Bmpr2*$^{-/-}$ mice were created in our laboratory as described (Spiekerkoetter et al., 2013). Endothelial SCL-CRE ERT mice, with a 5′-endothelial SCL enhancer (−7 to 0.9 kb) that directs expression to endothelium, were crossed with *Rosa26R* mice and with *Bmpr2*$^{fl/fl}$ mice created previously in our laboratory. Tamoxifen was given at 2mg/day i.p. for 10 days; after another 14 days, CRE activation was assessed and a deletion in *Bmpr2* in EC in lungs as well as all other vascularized tissues was observed. The number of mice per experiment is indicated in the figure legends. Mice (7–14 weeks of age) were housed in hypoxia (10% O_2) for three weeks and recovered for four weeks in room air, or housed in room air for seven weeks. Right ventricular systolic pressure and right ventricular hypertrophy (RVSP, RVH), cardiac function and output and pulmonary artery acceleration time (PAAT) were measured (Hansmann et al., 2008). The heart and lungs were perfused with PBS, the left lung fixed, and sections embedded in paraffin for immunohistochemistry and morphometry. The right lung was snap-frozen in liquid N_2, and kept at −80°C for protein and RNA extraction. For EC isolation, lungs were perfused with PBS, transferred to EC medium with 20% FBS and incubated at 37°. For SMC isolation, lungs were dissected directly after perfusion and pulmonary arteries were cleared of adventia and kept in cold HBSS before Elastase/Collagenase treatment.

Reagents and Cellular Assays—Commercial reagents and kits used for cellular assays are described in the Online Supplement.

Immunofluorescence—Sections from formaldehyde-fixed, paraffin-embedded mouse lungs were de-paraffinized and rehydrated. Epitope retrieval was performed and sections were then incubated with the primary antibodies against SMC Actin (1:1,000) and von Willebrand Factor (vWF) (1:50).

Tube formation assay—Cells were cultured in 5% FBS, and 10,000 cells were seeded on Matrigel. The number of tubes and tube length were assessed after 8h by light microscopy by two investigators blinded to the experimental group.

Migration by a Modified Boyden Chamber Assay—30,000 cells were seeded onto 0.2%-Gelatin-coated microporous inserts and cell migration assessed after 16h as described (Alastalo et al., 2011).

Cell Viability and Proliferation—PAEC exposed to hypoxia-reoxygenation were assessed for viability by propidium iodide staining and flow cytometry. Cell proliferation was assessed by BrdU incorporation into PAEC, measured using a colorimetric cell proliferation ELISA.

Cignal Reporter Assay—HEK-293T cells were transfected with NRF2 and p53 responsive luciferase constructs that encode the firefly luciferase reporter gene under the control of a promoter containing either the antioxidant response elements for NRF2 or the p53 response element. A *Renilla* construct encoding the *Renilla* luciferase reporter gene under the control of a CMV promoter was used as an internal control for normalizing transfection efficiencies and monitoring cell viability.

siRNA transfection—siRNA specific for human BMPR2, PGC1α, p53, NRF1, NRF2 and TFAM or siControl were transfected into PAEC by nucleofection or by lipofectamine. Knockdown efficiency was determined by immunoblotting or qPCR.

Caspase Assay—Cells were incubated for 1h in Caspase 3/7 Luciferase Reagent Mix and total luminescence was measured in a plate reader.

Western immunoblotting—Western immunoblotting was done as previously described (Sawada, 2014).

qRT-PCR—Total RNA was extracted and purified from cells. The quantity and quality of RNA were determined by a spectrophotometer, and then RNA was reverse transcribed to cDNA.

Mitochondrial Metabolism—Baseline mitochondrial function and mitochondrial stress response were measured by oxygen consumption rate (OCR) using the Cell Mito Stress Kit with an XF24 extracellular flux analyzer (SeaHorse Bioscience, North Billerica, MA).

Glycolytic capacity was measured using the XF Glycolysis Stress Test Kit (SeaHorse Bioscience) on the same device.

Mitochondrial Membrane Potential Assay—The mitochondrial membrane potential was determined using two fluorescent methods: the JC-1 dye (5′,6,6′-tetrachloro-1,1′,3,3′-tetraethylbenzimidazolylcarbocyanine iodide) assay and the TMRE (tetramethylrhodamine, ethyl ester) assay.

Dihydroethidium Staining—Production of reactive oxygen species (ROS) was evaluated by dihydroethidium staining.

Mitochondrial ROS assay—Murine lung EC were seeded onto live-cell imaging glass bottom dishes loaded with 100nM MitoTracker Green FM (Molecular Probes, Grand Island NY) to stain mitochondria, and 5μM MitoSOX Red (Molecular Probes) to detect mitochondrial superoxide. ROS production was normalized to cell number and mitochondrial content was calculated as the ratio of MitoSOX to MitoTracker fluorescence ($F_{MitoSOX/MitoTracker}$).

Mitochondrial Morphometry—The mitochondrial fragmentation index assessed by Mito Tracker was defined as ratio of fragmented mitochondria (dots) to tubular mitochondrial network branchpoints (rods) per total number of mitochondria/cell as determined by a semi-automated approach at the same contrast and brightness using Fiji software.

DNA isolation and PCR for Detection of mtDNA 4977bp Deletion—Total cellular DNA was isolated using DNeasy Blood and Tissue kit (Qiagen, Valencia CA) for PCR analysis. To detect the 4977bp deletion in mtDNA we used the following primers (Chen et al., 2011; Cheng et al., 2013): 1F, 5`-AACCACAGTTTCATGCCCATC-3; 1R, 5`-TGTTAGTAAGGGTGGGGAAGC-3`. The wild-type mtDNA primer sequences used were: F, 5`-GAAATGCCCCAACTAAATACCGT-3`; R, 5`-ATGAGTGAGGCAGGAGTCCG-3`. The presence of the 4977bp deletion was indicated by the appearance of a 352bp band (Chen et al., 2011), verified by sequencing analysis.

Detection of Free Mitochondrial DNA in Plasma of Mice—DNA was isolated from diluted plasma following centrifugation using DNeasy Blood and Tissue Kit (Qiagen). DNA was eluted, the DNA solution further diluted, and primers used to amplify mouse mitochondrial cytochrome oxidase related to nuclear DNA detected by 18S.

Statistical Analysis—All data are expressed as arithmetical mean±standard error of the mean (SEM). Statistical significance was determined first by two-way ANOVA followed by post hoc analysis (Bonferroni). So as not to overlook potentially important differences that were not judged to be significant by Bonferroni, we further subjected our data to the Newman Keul´s or Fisher LSD multiple comparison tests as indicated in the Figures and legends. Two-sided unpaired t-test analysis was used for comparison of two groups. A p-value of <0.05 was considered significant. The number of experiments, animals per group and the statistical test used are indicated in the figure legends.

Supplementary Material

Refer to Web version on PubMed Central for supplementary material.

Acknowledgments

References

Alastalo TP, Li M, Perez Vde J, Pham D, Sawada H, Wang JK, Koskenvuo M, Wang L, Freeman BA, Chang HY, et al. Disruption of PPARgamma/beta-catenin-mediated regulation of apelin impairs BMP-induced mouse and human pulmonary arterial EC survival. J Clin Invest. 2011; 121:3735–3746. [PubMed: 21821917]

Aquilano K, Baldelli S, Pagliei B, Cannata SM, Rotilio G, Ciriolo MR. p53 orchestrates the PGC-1alpha-mediated antioxidant response upon mild redox and metabolic imbalance. Antioxidants & redox signaling. 2013; 18:386–399. [PubMed: 22861165]

Archer SL, Gomberg-Maitland M, Maitland ML, Rich S, Garcia JG, Weir EK. Mitochondrial metabolism, redox signaling, and fusion: a mitochondria-ROS-HIF-1alpha-Kv1.5 O2-sensing pathway at the intersection of pulmonary hypertension and cancer. American journal of physiology Heart and circulatory physiology. 2008; 294:H570–H578. [PubMed: 18083891]

Archer SL, Marsboom G, Kim GH, Zhang HJ, Toth PT, Svensson EC, Dyck JR, Gomberg-Maitland M, Thebaud B, Husain AN, et al. Epigenetic attenuation of mitochondrial superoxide dismutase 2 in pulmonary arterial hypertension: a basis for excessive cell proliferation and a new therapeutic target. Circulation. 2010; 121:2661–2671. [PubMed: 20529999]

Atkinson C, Stewart S, Upton PD, Machado R, Thomson JR, Trembath RC, Morrell NW. Primary pulmonary hypertension is associated with reduced pulmonary vascular expression of type II bone morphogenetic protein receptor. Circulation. 2002; 105:1672–1678. [PubMed: 11940546]

Bonnet S, Michelakis ED, Porter CJ, Andrade-Navarro MA, Thebaud B, Bonnet S, Haromy A, Harry G, Moudgil R, McMurtry MS, et al. An abnormal mitochondrial-hypoxia inducible factor-1alpha-Kv channel pathway disrupts oxygen sensing and triggers pulmonary arterial hypertension in fawn hooded rats: similarities to human pulmonary arterial hypertension. Circulation. 2006; 113:2630–2641. [PubMed: 16735674]

Burton VJ, Holmes AM, Ciuclan LI, Robinson A, Roger JS, Jarai G, Pearce AC, Budd DC. Attenuation of leukocyte recruitment via CXCR1/2 inhibition stops the progression of PAH in mice with genetic ablation of endothelial BMPR-II. Blood. 2011; 118:4750–4758. [PubMed: 21900197]

Chen T, He J, Shen L, Fang H, Nie H, Jin T, Wei X, Xin Y, Jiang Y, Li H, et al. The mitochondrial DNA 4,977-bp deletion and its implication in copy number alteration in colorectal cancer. BMC Med Genet. 2011; 12:8. [PubMed: 21232124]

Cheng Y, Ren X, Gowda AS, Shan Y, Zhang L, Yuan YS, Patel R, Wu H, Huber-Keener K, Yang JW, et al. Interaction of Sirt3 with OGG1 contributes to repair of mitochondrial DNA and protects from apoptotic cell death under oxidative stress. Cell Death Dis. 2013; 4:e731. [PubMed: 23868064]

Chun HJ, Ali ZA, Kojima Y, Kundu RK, Sheikh AY, Agrawal R, Zheng L, Leeper NJ, Pearl NE, Patterson AJ, et al. Apelin signaling antagonizes Ang II effects in mouse models of atherosclerosis. J Clin Invest. 2008; 118:3343–3354. [PubMed: 18769630]

Culic O, Gruwel ML, Schrader J. Energy turnover of vascular endothelial cells. Am J Physiol. 1997; 273:C205–C213. [PubMed: 9252458]

Deng Z, Morse JH, Slager SL, Cuervo N, Moore KJ, Venetos G, Kalachikov S, Cayanis E, Fischer SG, Barst RJ, et al. Familial primary pulmonary hypertension (gene PPH1) is caused by mutations in the bone morphogenetic protein receptor-II gene. Am J Hum Genet. 2000; 67:737–744. [PubMed: 10903931]

Diebold I, Djordjevic T, Petry A, Hatzelmann A, Tenor H, Hess J, Gorlach A. Phosphodiesterase 2 mediates redox-sensitive endothelial cell proliferation and angiogenesis by thrombin via Rac1 and NADPH oxidase 2. Circ Res. 2009; 104:1169–1177. [PubMed: 19390057]

Duvezin-Caubet S, Jagasia R, Wagener J, Hofmann S, Trifunovic A, Hansson A, Chomyn A, Bauer MF, Attardi G, Larsson NG, et al. Proteolytic processing of OPA1 links mitochondrial dysfunction to alterations in mitochondrial morphology. J Biol Chem. 2006; 281:37972–37979. [PubMed: 17003040]

Fessel JP, Flynn CR, Robinson LJ, Penner NL, Gladson S, Kang CJ, Wasserman DH, Hemnes AR, West JD. Hyperoxia synergizes with mutant bone morphogenic protein receptor 2 to cause metabolic stress, oxidant injury, and pulmonary hypertension. American journal of respiratory cell and molecular biology. 2013; 49:778–787. [PubMed: 23742019]

Fijalkowska I, Xu W, Comhair SA, Janocha AJ, Mavrakis LA, Krishnamachary B, Zhen L, Mao T, Richter A, Erzurum SC, et al. Hypoxia inducible-factor1alpha regulates the metabolic shift of pulmonary hypertensive endothelial cells. Am J Pathol. 2010; 176:1130–1138. [PubMed: 20110409]

Frank S, Gaume B, Bergmann-Leitner ES, Leitner WW, Robert EG, Catez F, Smith CL, Youle RJ. The role of dynamin-related protein 1, a mediator of mitochondrial fission, in apoptosis. Developmental cell. 2001; 1:515–525. [PubMed: 11703942]

Giedt RJ, Yang C, Zweier JL, Matzavinos A, Alevriadou BR. Mitochondrial fission in endothelial cells after simulated ischemia/reperfusion: role of nitric oxide and reactive oxygen species. Free Radic Biol Med. 2012; 52:348–356. [PubMed: 22100972]

Gill SE, Taneja R, Rohan M, Wang L, Mehta S. Pulmonary microvascular albumin leak is associated with endothelial cell death in murine sepsis-induced lung injury in vivo. PLoS One. 2014; 9:e88501. [PubMed: 24516666]

Guignabert C, Alvira CM, Alastalo TP, Sawada H, Hansmann G, Zhao M, Wang L, El-Bizri N, Rabinovitch M. Tie2-mediated loss of peroxisome proliferator-activated receptor-gamma in mice causes PDGF receptor-beta-dependent pulmonary arterial muscularization. American journal of physiology Lung cellular and molecular physiology. 2009; 297:L1082–L1090. [PubMed: 19801450]

Hansmann G, de Jesus Perez VA, Alastalo TP, Alvira CM, Guignabert C, Bekker JM, Schellong S, Urashima T, Wang L, Morrell NW, et al. An antiproliferative BMP-2/PPARgamma/apoE axis in human and murine SMCs and its role in pulmonary hypertension. J Clin Invest. 2008; 118:1846–1857. [PubMed: 18382765]

Heo KS, Lee H, Nigro P, Thomas T, Le NT, Chang E, McClain C, Reinhart-King CA, King MR, Berk BC, et al. PKCzeta mediates disturbed flow-induced endothelial apoptosis via p53 SUMOylation. J Cell Biol. 2011; 193:867–884. [PubMed: 21624955]

Howe JR, Bair JL, Sayed MG, Anderson ME, Mitros FA, Petersen GM, Velculescu VE, Traverso G, Vogelstein B. Germline mutations of the gene encoding bone morphogenetic protein receptor 1A in juvenile polyposis. Nat Genet. 2001; 28:184–187. [PubMed: 11381269]

Jilwan FN, Escourrou P, Garcia G, Jais X, Humbert M, Roisman G. High occurrence of hypoxemic sleep respiratory disorders in precapillary pulmonary hypertension and mechanisms. Chest. 2013; 143:47–55. [PubMed: 22878784]

Julian MW, Shao G, Vangundy ZC, Papenfuss TL, Crouser ED. Mitochondrial transcription factor A, an endogenous danger signal, promotes TNFalpha release via RAGE- and TLR9-responsive plasmacytoid dendritic cells. PLoS One. 2013; 8:e72354. [PubMed: 23951313]

Kim J, Kang Y, Kojima Y, Lighthouse JK, Hu X, Aldred MA, McLean DL, Park H, Comhair SA, Greif DM, et al. An endothelial apelin-FGF link mediated by miR-424 and miR-503 is disrupted in pulmonary arterial hypertension. Nature medicine. 2013; 19:74–82.

Kim YM, Haghighat L, Spiekerkoetter E, Sawada H, Alvira CM, Wang L, Acharya S, Rodriguez-Colon G, Orton A, Zhao M, et al. Neutrophil elastase is produced by pulmonary artery smooth

muscle cells and is linked to neointimal lesions. The American journal of pathology. 2011; 179:1560–1572. [PubMed: 21763677]

Lane KB, Machado RD, Pauciulo MW, Thomson JR, Phillips JA 3rd, Loyd JE, Nichols WC, Trembath RC. Heterozygous germline mutations in BMPR2, encoding a TGF-beta receptor, cause familial primary pulmonary hypertension. Nature genetics. 2000; 26:81–84. [PubMed: 10973254]

Lane KL, Talati M, Austin E, Hemnes AR, Johnson JA, Fessel JP, Blackwell T, Mernaugh RL, Robinson L, Fike C, et al. Oxidative injury is a common consequence of BMPR2 mutations. Pulm Circ. 2011; 1:72–83. [PubMed: 21904662]

Larsson NG, Wang J, Wilhelmsson H, Oldfors A, Rustin P, Lewandoski M, Barsh GS, Clayton DA. Mitochondrial transcription factor A is necessary for mtDNA maintenance and embryogenesis in mice. Nat Genet. 1998; 18:231–236. [PubMed: 9500544]

Li M, Riddle SR, Frid MG, El Kasmi KC, McKinsey TA, Sokol RJ, Strassheim D, Meyrick B, Yeager ME, Flockton AR, et al. Emergence of fibroblasts with a proinflammatory epigenetically altered phenotype in severe hypoxic pulmonary hypertension. J Immunol. 2011; 187:2711–2722. [PubMed: 21813768]

Masri FA, Xu W, Comhair SA, Asosingh K, Koo M, Vasanji A, Drazba J, Anand-Apte B, Erzurum SC. Hyperproliferative apoptosis-resistant endothelial cells in idiopathic pulmonary arterial hypertension. Am J Physiol Lung Cell Mol Physiol. 2007; 293:L548–L554. [PubMed: 17526595]

Matuschak GM, Munoz CF, Johanns CA, Rahman R, Lechner AJ. Upregulation of postbacteremic TNF-alpha and IL-1alpha gene expression by alveolar hypoxia/reoxygenation in perfused rat lungs. Am J Respir Crit Care Med. 1998; 157:629–637. [PubMed: 9476882]

McMurtry MS, Bonnet S, Wu X, Dyck JR, Haromy A, Hashimoto K, Michelakis ED. Dichloroacetate prevents and reverses pulmonary hypertension by inducing pulmonary artery smooth muscle cell apoptosis. Circulation research. 2004; 95:830–840. [PubMed: 15375007]

Michelakis ED, Hampl V, Nsair A, Wu X, Harry G, Haromy A, Gurtu R, Archer SL. Diversity in mitochondrial function explains differences in vascular oxygen sensing. Circ Res. 2002a; 90:1307–1315. [PubMed: 12089069]

Michelakis ED, McMurtry MS, Wu XC, Dyck JR, Moudgil R, Hopkins TA, Lopaschuk GD, Puttagunta L, Waite R, Archer SL. Dichloroacetate, a metabolic modulator, prevents and reverses chronic hypoxic pulmonary hypertension in rats: role of increased expression and activity of voltage-gated potassium channels. Circulation. 2002b; 105:244–250. [PubMed: 11790708]

Mizuno S, Bogaard HJ, Kraskauskas D, Alhussaini A, Gomez-Arroyo J, Voelkel NF, Ishizaki T. p53 Gene deficiency promotes hypoxia-induced pulmonary hypertension and vascular remodeling in mice. American journal of physiology Lung cellular and molecular physiology. 2011; 300:L753–L761. [PubMed: 21335523]

Mouraret N, Marcos E, Abid S, Gary-Bobo G, Saker M, Houssaini A, Dubois-Rande JL, Boyer L, Boczkowski J, Derumeaux G, et al. Activation of lung p53 by Nutlin-3a prevents and reverses experimental pulmonary hypertension. Circulation. 2013; 127:1664–1676. [PubMed: 23513067]

Park KH, Lee TH, Kim CW, Kim J. Enhancement of CCL15 expression and monocyte adhesion to endothelial cells (ECs) after hypoxia/reoxygenation and induction of ICAM-1 expression by CCL15 via the JAK2/STAT3 pathway in ECs. J Immunol. 2013; 190:6550–6558. [PubMed: 23690481]

Potus F, Malenfant S, Graydon C, Mainguy V, Tremblay E, Breuils-Bonnet S, Ribeiro F, Porlier A, Maltais F, Bonnet S, et al. Impaired angiogenesis and peripheral muscle microcirculation loss contribute to exercise intolerance in pulmonary arterial hypertension. Am J Respir Crit Care Med. 2014; 190:318–328. [PubMed: 24977625]

Rabinovitch M, Gamble WJ, Miettinen OS, Reid L. Age and sex influence on pulmonary hypertension of chronic hypoxia on recovery. Am J Physiol. 1981; 240:H62–H72. [PubMed: 6450541]

Rowe GC, Jiang A, Arany Z. PGC-1 coactivators in cardiac development and disease. Circ Res. 2010; 107:825–838. [PubMed: 20884884]

Ryan JJ, Marsboom G, Fang YH, Toth PT, Morrow E, Luo N, Piao L, Hong Z, Ericson K, Zhang HJ, et al. PGC1alpha-mediated mitofusin-2 deficiency in female rats and humans with pulmonary arterial hypertension. Am J Respir Crit Care Med. 2013; 187:865–878. [PubMed: 23449689]

Sakao S, Tatsumi K, Voelkel NF. Endothelial cells and pulmonary arterial hypertension: apoptosis, proliferation, interaction and transdifferentiation. Respir Res. 2009; 10:95. [PubMed: 19825167]

Sawada H, Saito T, Nickel NP, Alastalo TP, Glotzbach JP, Chan R, Haghighat L, Fuchs G, Januszyk M, Cao A, et al. Reduced BMPR2 expression induces GM-CSF translation and macrophage recruitment in humans and mice to exacerbate pulmonary hypertension. J Exp Med. 2014a; 211:263–280. [PubMed: 24446489]

Sawada N, Jiang A, Takizawa F, Safdar A, Manika A, Tesmenitsky Y, Kang KT, Bischoff J, Kalwa H, Sartoretto JL, et al. Endothelial PGC-1alpha Mediates Vascular Dysfunction in Diabetes. Cell metabolism. 2014b; 19:246–258. [PubMed: 24506866]

Shimasaki Y, Pan N, Messina LM, Li C, Chen K, Liu L, Cooper MP, Vita JA, Keaney JF Jr. Uncoupling protein 2 impacts endothelial phenotype via p53-mediated control of mitochondrial dynamics. Circulation research. 2013; 113:891–901. [PubMed: 23819990]

Spiekerkoetter E, Tian X, Cai J, Hopper RK, Sudheendra D, Li CG, El-Bizri N, Sawada H, Haghighat R, Chan R, et al. FK506 activates BMPR2, rescues endothelial dysfunction, and reverses pulmonary hypertension. J Clin Invest. 2013; 123:3600–3613. [PubMed: 23867624]

Sutendra G, Bonnet S, Rochefort G, Haromy A, Folmes KD, Lopaschuk GD, Dyck JR, Michelakis ED. Fatty acid oxidation and malonyl-CoA decarboxylase in the vascular remodeling of pulmonary hypertension. Sci Transl Med. 2010; 2 44ra58.

Sutendra G, Dromparis P, Bonnet S, Haromy A, McMurtry MS, Bleackley RC, Michelakis ED. Pyruvate dehydrogenase inhibition by the inflammatory cytokine TNFalpha contributes to the pathogenesis of pulmonary arterial hypertension. J Mol Med (Berl). 2011; 89:771–783. [PubMed: 21809123]

Sutendra G, Michelakis ED. The Metabolic Basis of Pulmonary Arterial Hypertension. Cell metabolism. 2014

Taylor RW, Turnbull DM. Mitochondrial DNA mutations in human disease. Nat Rev Genet. 2005; 6:389–402. [PubMed: 15861210]

Teichert-Kuliszewska K, Kutryk MJ, Kuliszewski MA, Karoubi G, Courtman DW, Zucco L, Granton J, Stewart DJ. Bone morphogenetic protein receptor-2 signaling promotes pulmonary arterial endothelial cell survival: implications for loss-of-function mutations in the pathogenesis of pulmonary hypertension. Circulation research. 2006; 98:209–217. [PubMed: 16357305]

Urboniene D, Haber I, Fang YH, Thenappan T, Archer SL. Validation of high-resolution echocardiography and magnetic resonance imaging vs. high-fidelity catheterization in experimental pulmonary hypertension. American journal of physiology Lung cellular and molecular physiology. 2010; 299:L401–L412. [PubMed: 20581101]

Villeneuve C, Guilbeau-Frugier C, Sicard P, Lairez O, Ordener C, Duparc T, De Paulis D, Couderc B, Spreux-Varoquaux O, Tortosa F, et al. p53-PGC-1alpha pathway mediates oxidative mitochondrial damage and cardiomyocyte necrosis induced by monoamine oxidase-A upregulation: role in chronic left ventricular dysfunction in mice. Antioxid Redox Signal. 2013; 18:5–18. [PubMed: 22738191]

Virbasius JV, Scarpulla RC. Activation of the human mitochondrial transcription factor A gene by nuclear respiratory factors: a potential regulatory link between nuclear and mitochondrial gene expression in organelle biogenesis. Proc Natl Acad Sci U S A. 1994; 91:1309–1313. [PubMed: 8108407]

West AP, Shadel GS, Ghosh S. Mitochondria in innate immune responses. Nature reviews Immunology. 2011; 11:389–402.

Xu W, Koeck T, Lara AR, Neumann D, Difilippo FP, Koo M, Janocha AJ, Masri FA, Arroliga AC, Jennings C, et al. Alterations of cellular bioenergetics in pulmonary artery endothelial cells. Proc Natl Acad Sci U S A. 2007; 104:1342–1347. [PubMed: 17227868]

Zhang Q, Raoof M, Chen Y, Sumi Y, Sursal T, Junger W, Brohi K, Itagaki K, Hauser CJ. Circulating mitochondrial DAMPs cause inflammatory responses to injury. Nature. 2010; 464:104–107. [PubMed: 20203610]
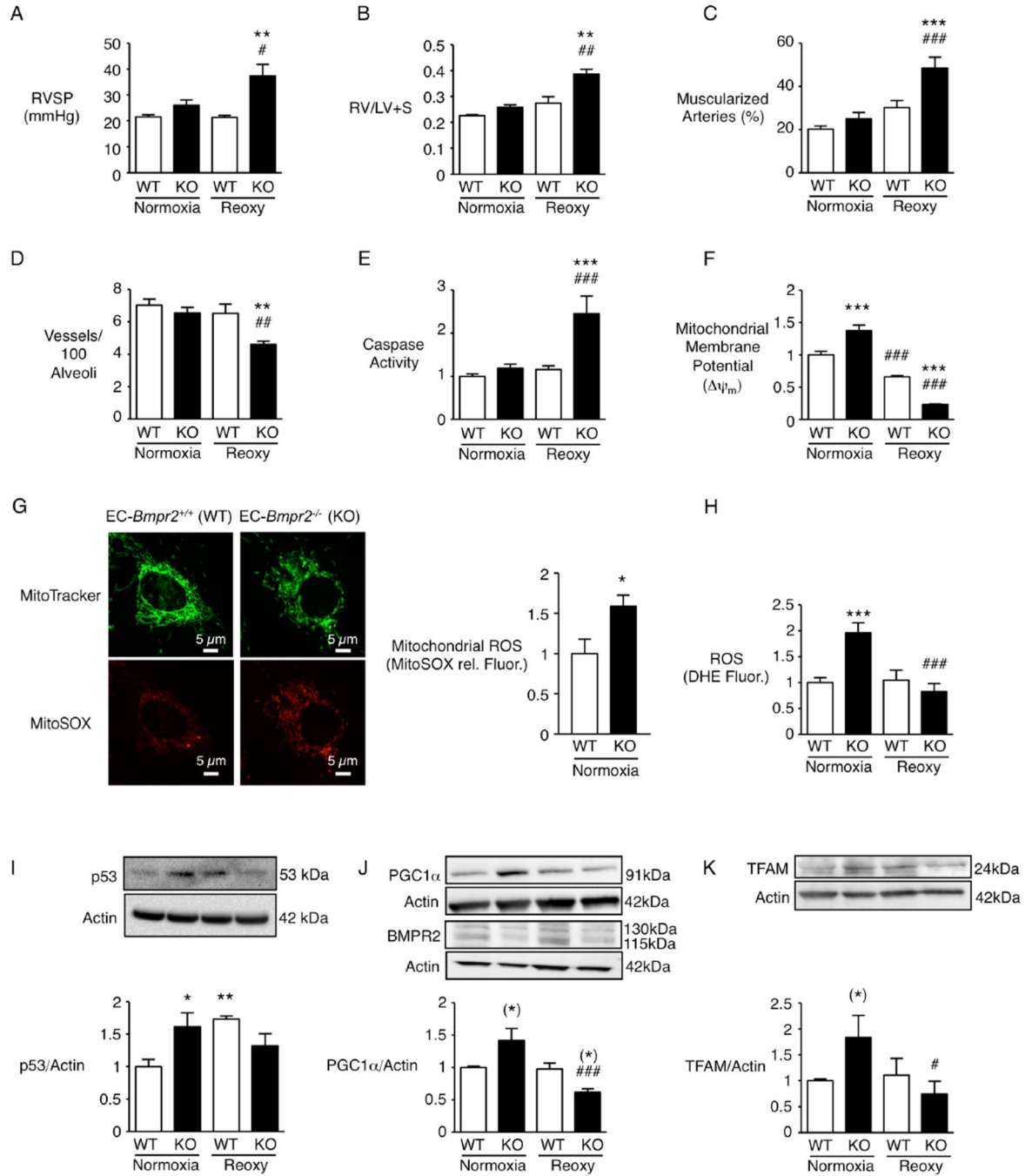
Figure 1. EC-Bmpr2⁻/⁻ mice show unresolved pulmonary hypertension

*EC-Bmpr2⁻/⁻ (*KO) vs. littermate wild type (WT) mice were exposed to three weeks of hypoxia (10% O_2) and four weeks reoxygenation in normoxia (hypoxia-reoxygenation, Reoxy), or housed for seven weeks in normoxia. We measured **(A)** right ventricular systolic pressure (RVSP), **(B)** right ventricular (RV) hypertrophy (weight of RV/left ventricle and septum) (RV/LV+S), **(C)** muscularization of pulmonary arteries, % of fully or partially muscularized arteries, at alveolar wall and duct level **(D)** arteries at alveolar duct and wall level per 100 alveoli. **(E–K)** Lung endothelial cells were isolated from these mice and **(E)**

apoptosis assessed by caspase3/7 luminescence assay, **(F)** mitochondrial membrane potential (ψ_m) using the TMRE fluorescence probe, **(G)** mitochondrial ROS generation by MitoSOX **(H)**, total reactive oxygen species (ROS) by dihydroethidium (DHE). Representative immunoblots and relative densitometric analysis of **(I)** p53, **(J)** PGC1α and BMPR2, and **(K)** TFAM with β-Actin as loading control. Bars=Mean±SEM of (A) n=5, WT/KO normoxia; n=7, WT Reoxy, n=10, KO Reoxy, (B) n=4, WT; n=3, KO normoxia ; n=5, WT Reoxy; n=7, KO Reoxy; (C–G) n=3; (H) n=9; (I) n=6; (J) n=5, (K) n=4. *, **, ***, $P<0.05$, <0.01 and <0.001 comparing genotypes under the same condition, and #, ## and ###, $P<0.05$, <0.01 and <0.001 comparing the same genotype across conditions. Analyses performed by two-way ANOVA and Bonferonni post-hoc or, as indicated by (), Neuman-Keuls. See also Fig. S1.
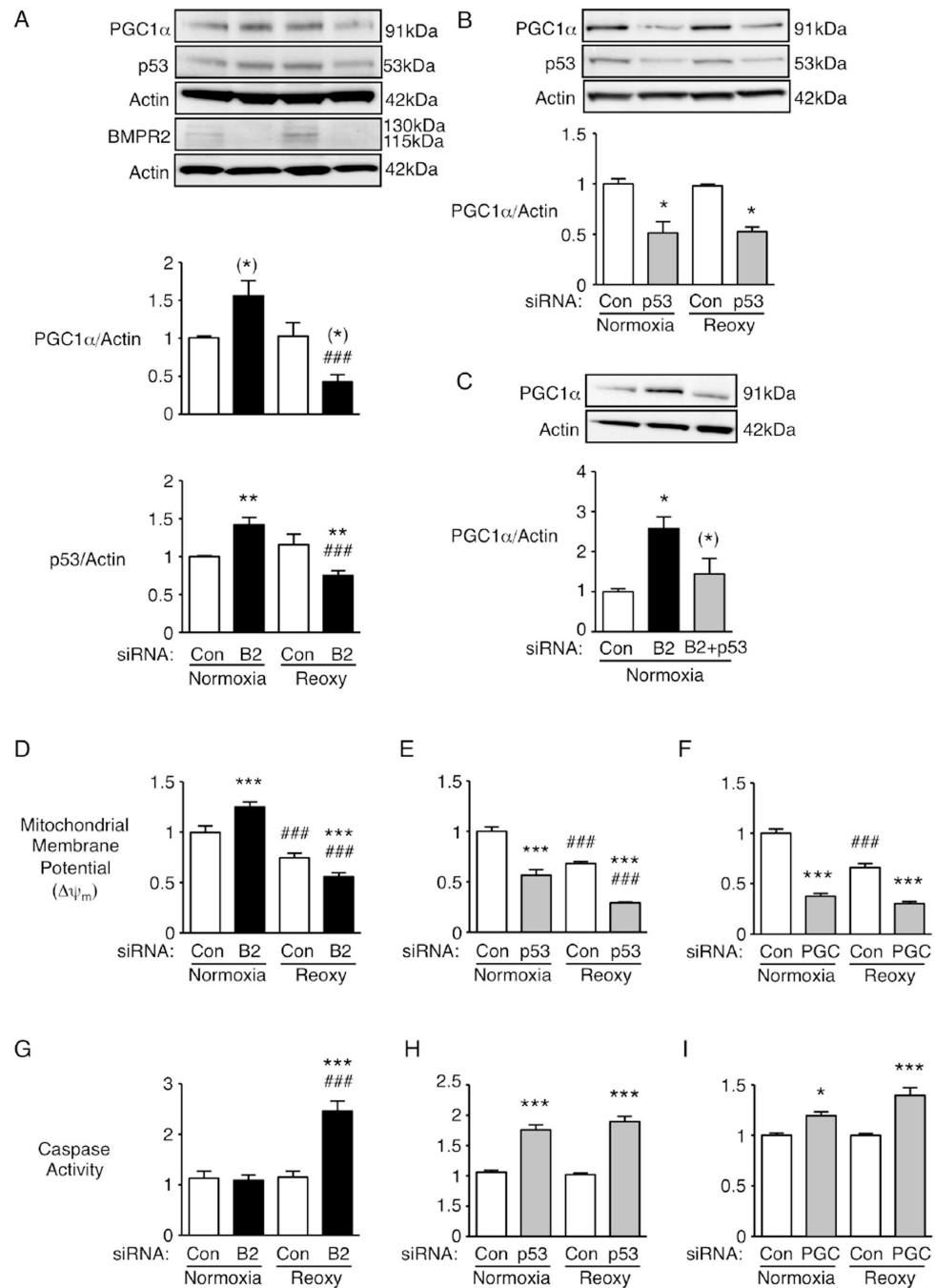
Figure 2. BMPR2 regulates p53 and PGC1α

Representative immunoblots and densitometry of commercially available human PAEC transfected with (**A**) BMPR2 (B2) siRNA, (**B**) p53 siRNA or (**C**) B2 and p53 siRNA or non-targeting (Con) siRNA and exposed to hypoxia (0.5% O_2) for 48h followed by normoxia (21% O_2) for 48h, i.e., hypoxia-reoxygenation (Reoxy), or incubated in normoxia (21% O_2) for 96h. (**D–F**) ψ_m in PAEC transfected with (**D**) B2 siRNA, (**E**) p53 siRNA and (**F**) PGC1α (PGC) siRNA vs. Con siRNA was measured by fluorescence probes, JC-1 (**D, F**) or TMRE (**E**). (**G–I**) Caspase3/7 luminescence measured in PAEC transfected with (**G**) B2,

(H) p53 or **(I)** PGC1α siRNA vs. non-targeting (Con) siRNA. Bars=Mean±SEM of (A) n=5, (B–H) n=3 and (I) n=4. Analyses as in legend to Fig. 1, () reflects Tukey or Neuman-Keuls post hoc test. See also Fig. S2.
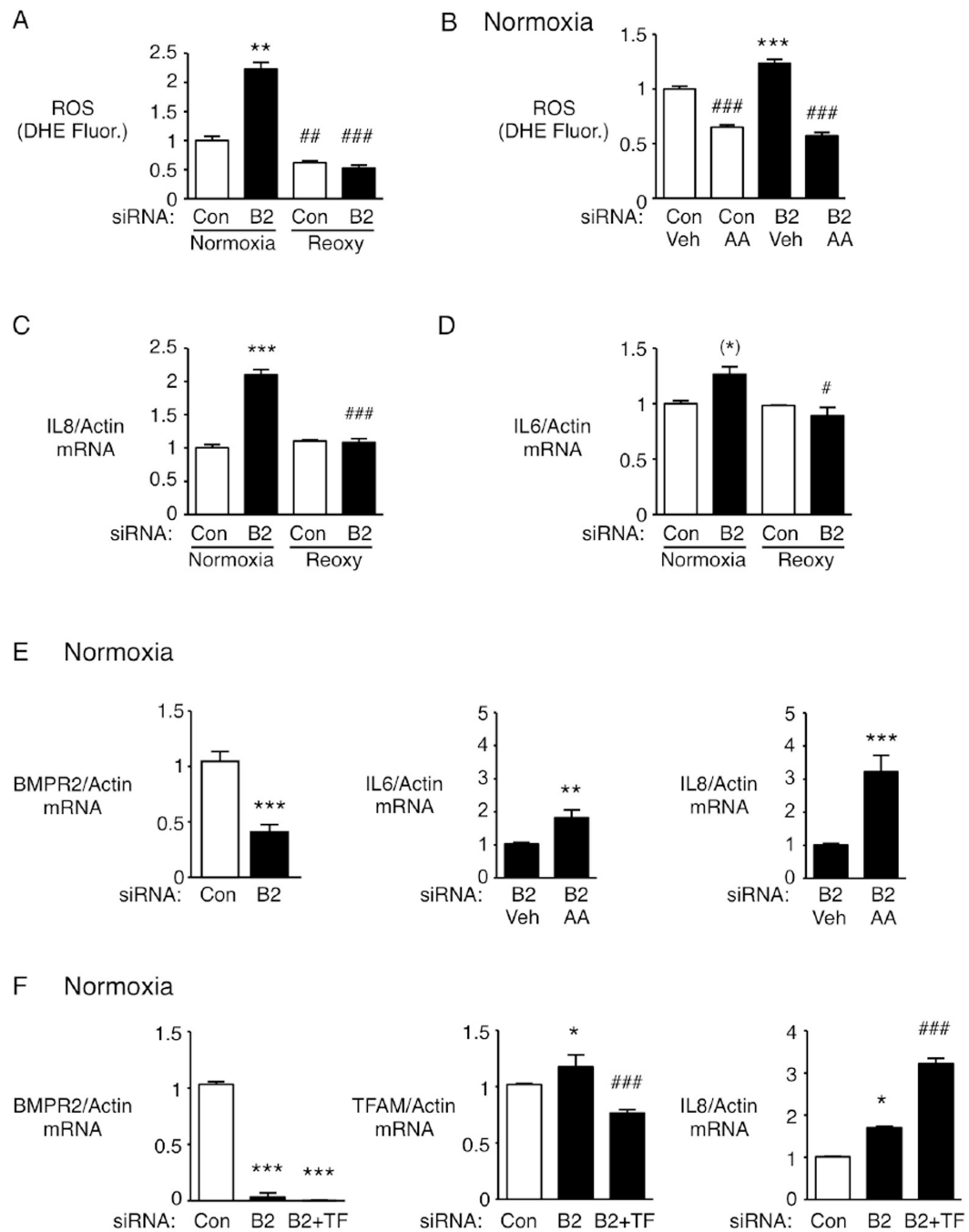
Figure 3. Reducing BMPR2 in normoxia induces an inflammatory response

PAEC were transfected with B2 or Con siRNA in normoxia and hypoxia-reoxygenation (Reoxy) as described for Fig. 2. **(A)** ROS measured by DHE fluorescence. **(B)** ROS production by PAEC transfected with B2 or Con siRNA and treated with Antimycin (AA, 10μM) or vehicle (Veh) for 1h in normoxia. **(C)** IL8 mRNA and **(D)** IL6 mRNA. **(E)** BMPR2, IL6 and IL8 mRNA, of PAEC transfected with B2 or Con siRNA under normoxia and AA treatment as in B. **(F)** BMPR2, TFAM and IL8 mRNA levels, of PAEC transfected

with B2 siRNA or B2+TFAM siRNA. All mRNA normalized to β-Actin, Bars=Mean±SEM of n=3 with analyses as in Fig. 1 and 2.
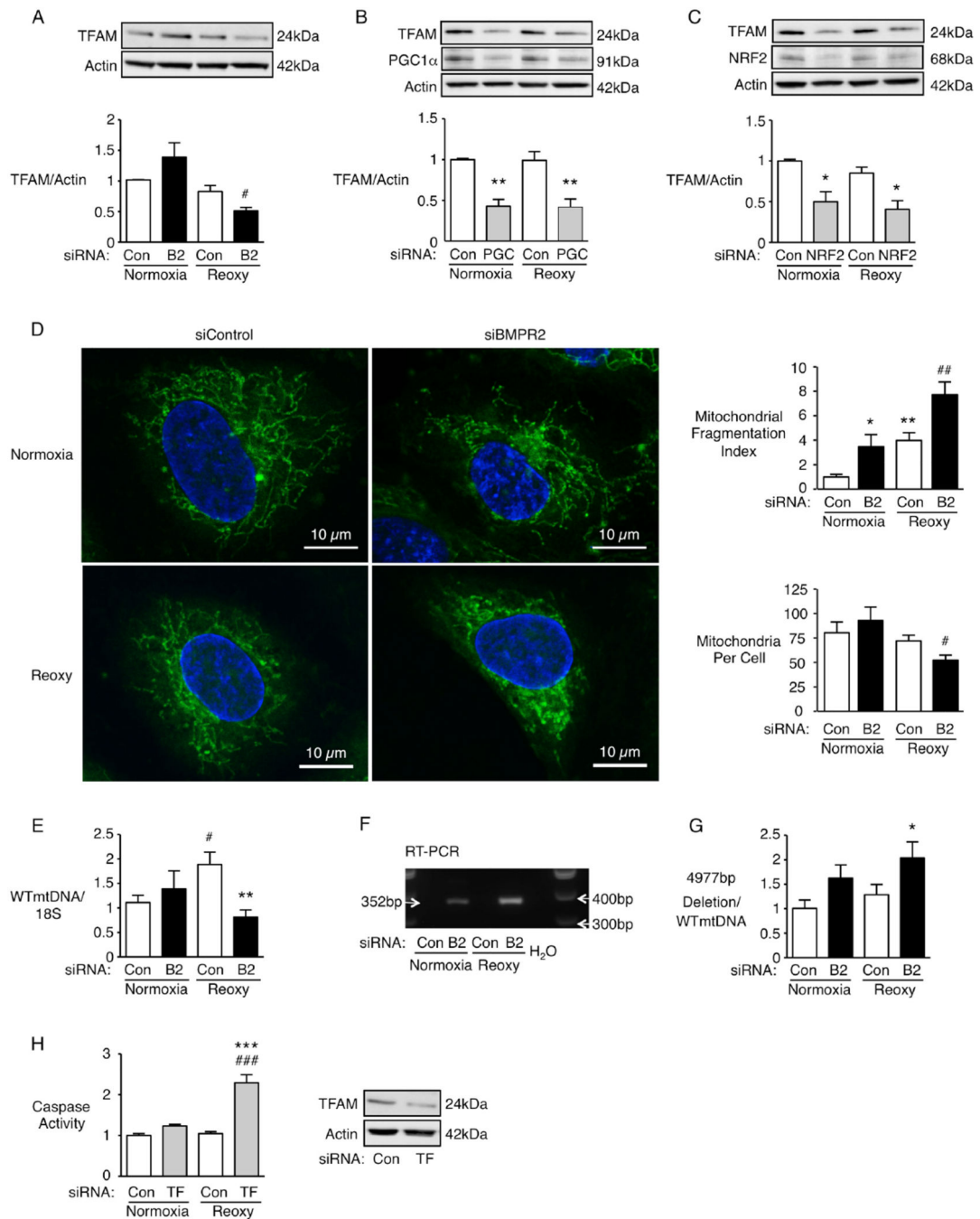
Figure 4. Reducing BMPR2 causes mtDNA deletion during hypoxia-reoxygenation related to reduced TFAM and elevated caspase activity

Representative immunoblots and densitometry for TFAM in PAEC transfected under normoxia or hypoxia-reoxygenation (Reoxy) with **(A)** B2 **(B)** PGC1α (PGC) and **(C)** NRF2 siRNA, vs. Con siRNA. **(D)** Confocal images of mitochondrial morphology, fragmentation index and total number as determined by MitoTracker Green staining under conditions of **A.** **(E)** Total mtDNA/nuclear DNA (18S). mtDNA 4977bp deletion shown as a 352bp amplicon on a 2% agarose gel **(F)** detected by q-RT-PCR **(G)** after transfection of B2 siRNA. **(H)**

PAEC transfected with TFAM (TF) vs. Con siRNA. Representative immunoblot on right and apoptosis assessed by caspase activity under normoxia and Reoxy. Bars=Mean±SEM of n=3 with analyses as in Fig. 1. See also Supp. Fig. S3.
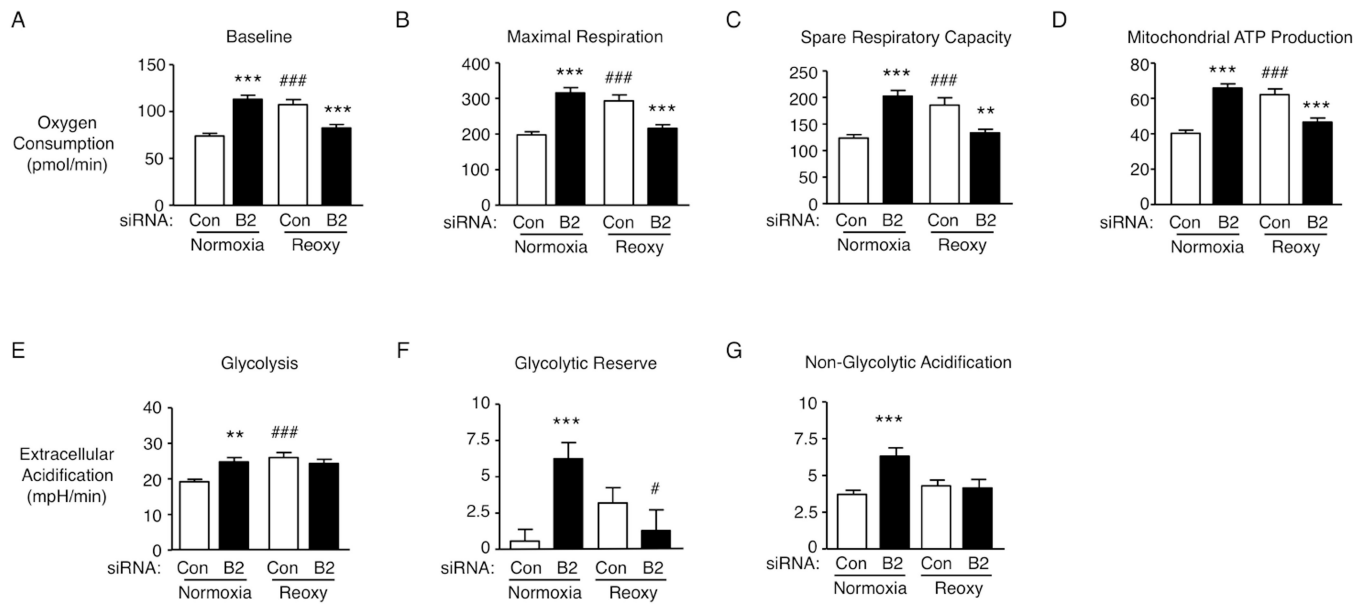
Figure 5. Loss of BMPR2 alters mitochondrial function and glucose utilization of pulmonary artery endothelial cells
Oxygen consumption rates of human PAEC transfected with B2 siRNA or non-targeting (Con) siRNA as described in Fig 2. **(A)** baseline and **(B)** maximal respiration following FCCP treatment, **(C)** Spare respiratory capacity and **(D)** derived mitochondrial ATP production. Extracellular acidification rates were measured to determine **(E)** aerobic glycolysis and **(F)** glycolytic reserve after sequential treatment with 10mM Glucose and 1μM Oligomycin. **(G)** Non-glycolytic acidification after treatment with 100mM 2-Deoxyglucose under the same conditions. Bars=Mean±SEM of (A–G) n=3 with analyses as in Fig. 1.
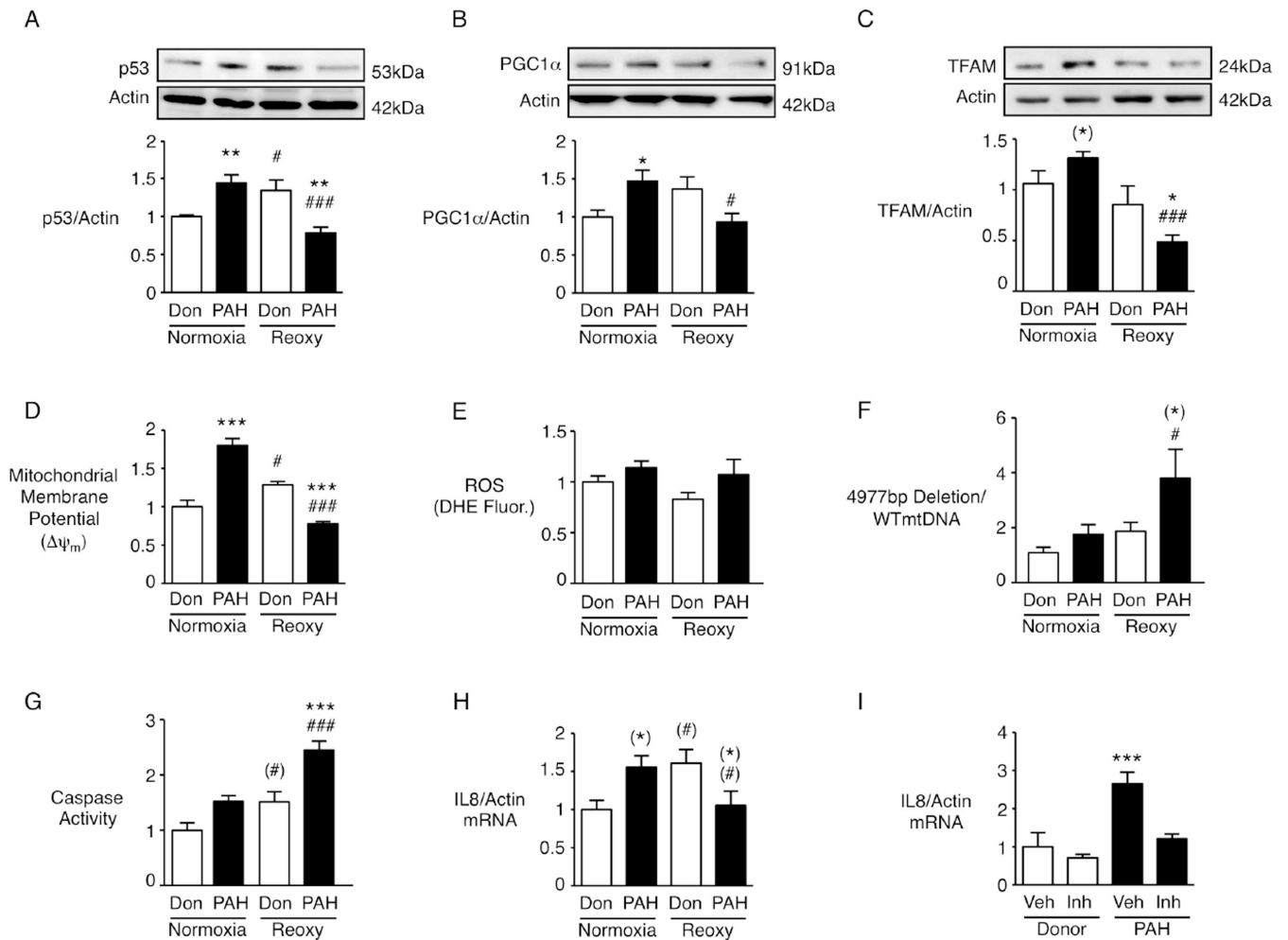
Figure 6. Pulmonary artery endothelial cells from patients with pulmonary arterial hypertension recapitulate the pro-inflammatory state in normoxia, and the pro-apoptotic state with hypoxia-reoxygenation

PAEC from patients (PAH) or unused donors (Don) lungs as controls were incubated in normoxia or following the hypoxia-reoxygenation protocol (Reoxy). **(A–C)** Representative immunoblots and quantitative densitometry with β-Actin as loading control for p53 **(A)**, PGC1α **(B)** and TFAM **(C). (D)** mitochondrial membrane activity by JC-1, **(E)** ROS production by DHE fluorescence (DHE Fluor), **(F)** the amplicon representing the 4977bp mtDNA deletion, and **(G)** apoptosis by caspase activity. qRT-PCR for IL8 is shown in **(H)** and **(I)**. To assess activation of IL8 by TLR-9, the inhibitor (inh, ODN TTAGG) or vehicle (veh) was used in donor and in PAH PAEC under normoxia **(I)**. Bars=Mean±SEM, n=3. Analyses as in Fig. 1 with () indicating significance by Neuman-Keuls (C, F, G) or by Fisher LSD (H).

WORKING MODEL
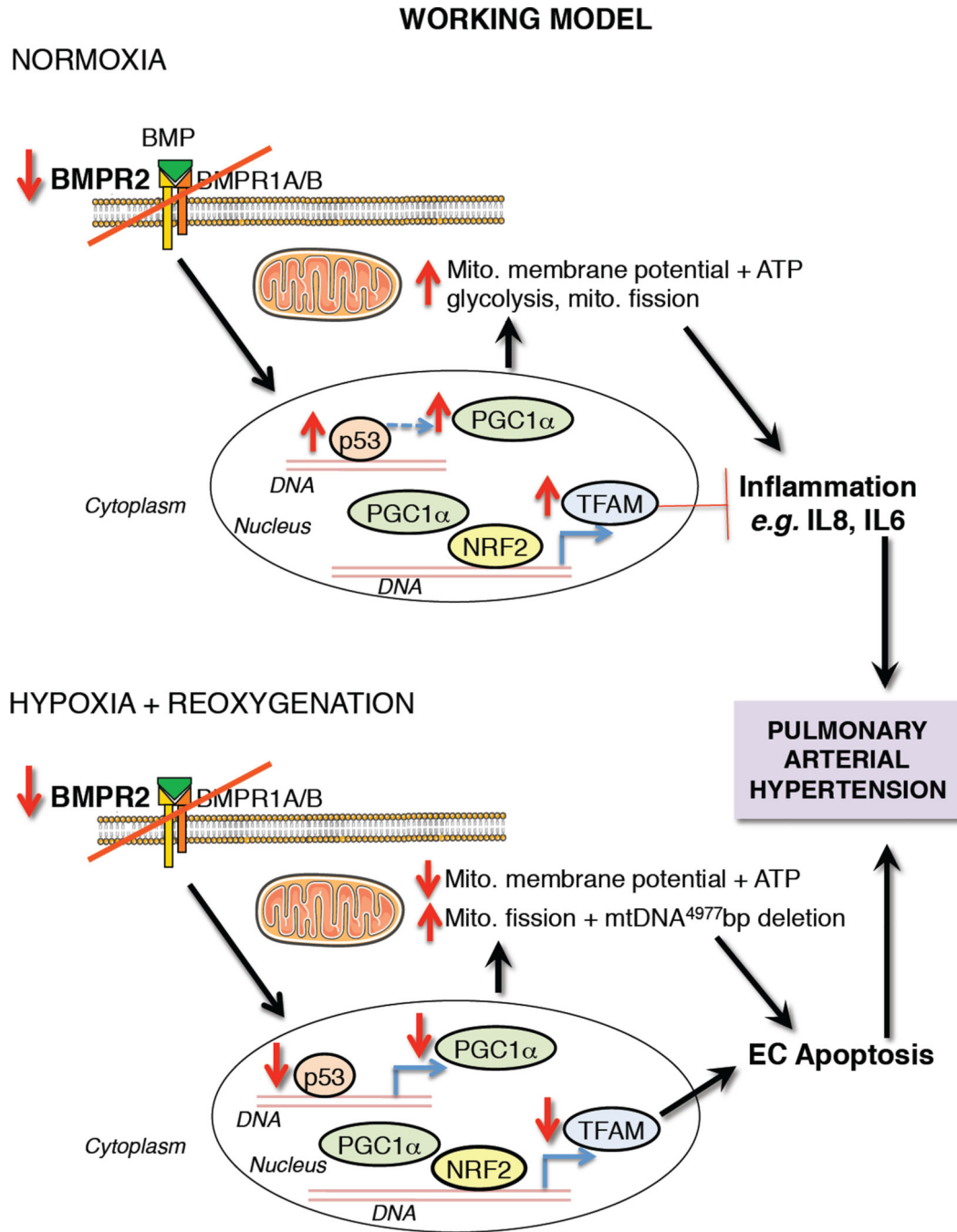
NORMOXIA

HYPOXIA + REOXYGENATION

Figure 7. Working model: A link between BMPR2-signaling and mitochondrial function
Loss of BMPR2 in PAEC during normoxia enhances mitochondrial biogenesis, driven by p53 PGC1α, NRF2 and TFAM, increases ψ_m and ATP, and glycolysis, leading to fission and causing a pro-inflammatory state via Interleukins such as IL8. The increase in TFAM appears to partially mitigate the increase in IL8. Loss of BMPR2 during reoxygenation after hypoxia impairs p53-dependent regulation of PGC1α and TFAM, reduces ψ_m and ATP and causes mitochondrial fission and mitochondrial DNA deletion, inducing PAEC apoptosis leading to loss of microvessels and aberrant proliferation of SM-like cells. Both

inflammation and EC apoptosis contribute to pulmonary arterial hypertension (Red arrows indicate up or down regulation; black arrows, sequalea).